ACS OMEGA

Open Access

http://pubs.acs.org/journal/acsodf

Article

Enhancing Immune Responses against SARS-CoV-2 Variants in Aged Mice with INDUK: A Chimeric DNA Vaccine Encoding the Spike S1-TM Subunits

Lishan Cui, Junbiao Wang, Fiorenza Orlando, Robertina Giacconi, Marco Malavolta, Beatrice Bartozzi, Roberta Galeazzi, Giorgia Giorgini, Luca Pesce, Francesco Cardarelli, Erica Quagliarini, Serena Renzi, Siyao Xiao, Daniela Pozzi,* Mauro Provinciali, Giulio Caracciolo, Cristina Marchini,* and Augusto Amici

Cite This: *ACS Omega* 2024, 9, 34624−34635

Read Online

ACCESS | Metrics & More | Article Recommendations | Supporting Information

ABSTRACT: Currently available vaccines against COVID-19 showed high efficacy against the original strain of SARS-CoV-2 but progressively lower efficacy against new variants. In response to emerging SARS-CoV-2 strains, we propose chimeric DNA vaccines encoding the spike antigen, including a combination of selected key mutations from different variants of concern. We developed two DNA vaccines, pVAX-S1-TM-D614G and pVAX-S1-TM-INDUK (INDUK), encoding the SARS-CoV-2 S1 spike subunit in fusion with the transmembrane region that allows protein trimerization as predicted by *in silico* analysis. pVAX-S1-TM-D614G included the dominant D614G substitution, while the chimeric vaccine INDUK contained additional selected mutations from the Delta (E484Q and L452R) and Alpha (N501Y and A570D) variants. Considering that aging is a risk factor for severe disease and that suboptimal vaccine responses were observed in older individuals, the immunogenicity of pVAX-S1-TM-D614G and INDUK was tested in both young and aged C57BL/6 mice. Two vaccine doses were able to trigger significant anti-SARS-CoV-2 antibody production, showing neutralizing activity. ELISA tests confirmed that antibodies induced by pVAX-S1-TM-D614G and INDUK were able to recognize both Wuhan Spike and Delta variant Spike as trimers, while neutralizing antibodies were detected by an ACE2:SARS-CoV-2 Spike S1 inhibitor screening assay, designed to assess the capacity of antibodies to block the interaction between the viral spike S1 protein and the ACE2 receptor. Although antibody titer declined within six months, a third booster dose significantly increased the magnitude of humoral response, even in aged individuals, suggesting that immune recall can improve antibody response durability. The analysis of cellular responses demonstrated that vaccination with INDUK elicited an increase in the percentage of SARS-CoV-2-specific IFN-γ producing T lymphocytes in immunized young mice and TNF-α-producing T lymphocytes in both young and aged mice. These findings not only hold immediate promise for addressing evolving challenges in SARS-CoV-2 vaccination but also open avenues to refine strategies and elevate the effectiveness of next-generation vaccines.

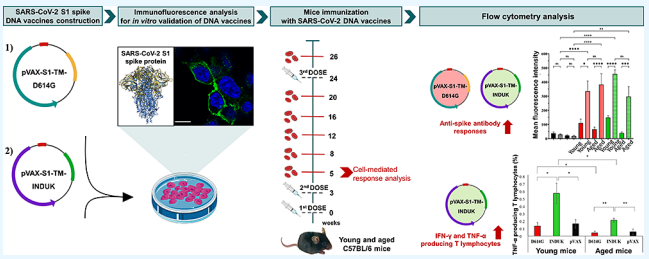

INTRODUCTION

In December 2019, the world witnessed the emergence of severe acute respiratory syndrome coronavirus 2 (SARS-CoV-2), marking the onset of a global pandemic.[1] The swift spread of the virus prompted the World Health Organization (WHO) to declare the COVID-19 outbreak an international public health emergency on January 30, 2020.[2] Although vaccines against SARS-CoV-2 saved millions of lives in these last three years, their effectiveness inevitably decreased against various emerging SARS-CoV-2 variants, such as B.1.1.7 (Alpha), B.1.351 (Beta), and B.1.617.2 (Delta) and the currently circulating Omicron variants, which caused continuing waves of infections.[3] Thus, the development of optimized vaccines, able to elicit protection against the new strains of the virus, is mandatory. The Spike (S) glycoprotein of the SARS-CoV-2 is an ideal target for vaccine design because it associates with the human angiotensin-converting enzyme 2 (ACE2) receptor to permit viral entry.[4] The S protein consists of two subunits (S1 and S2). The S1 subunit can be further defined with two domains termed the N-terminal domain (NTD) and the C-terminal domain (CTD), which includes the receptor-binding domain (RBD).[5] Currently, SARS-CoV-2 spike protein-encoding nucleic acid vaccines are considered to be the most effective vaccines against COVID-19. In particular, mRNA vaccines, such as mRNA-1273/SpikeVax by Moderna and

Received: April 5, 2024
Revised: June 12, 2024
Accepted: June 14, 2024
Published: July 30, 2024

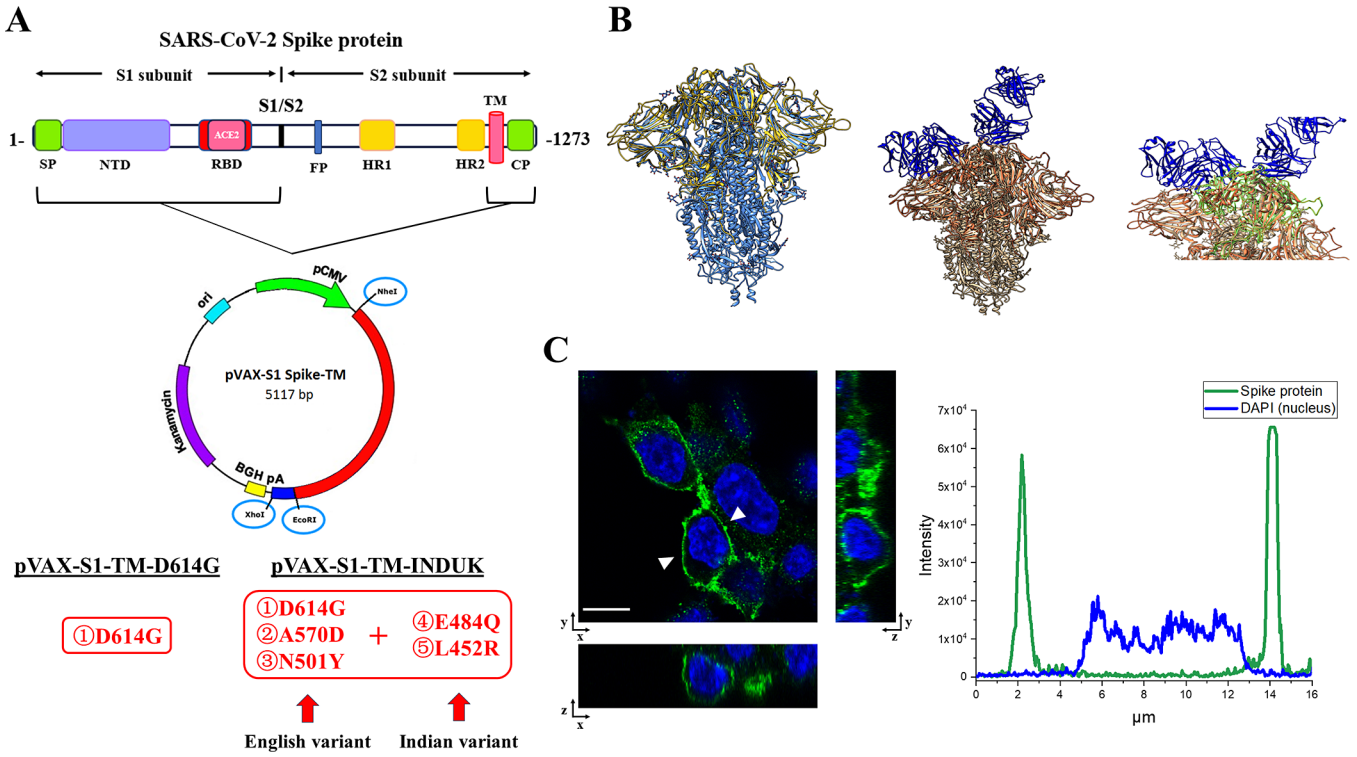

Figure 1. (A) Schematic diagram of the pVAX-Spike-S1-TM map and schematic representation of the domain arrangement of the SARS-CoV-2 S protein precursor. SP, signal peptide; NTD: N-terminal domain; RBD: receptor-binding domain; FP, fusion peptide; HR1, heptad repeat 1; HR2, heptad repeat 2; TM, transmembrane domain; CP, cytoplasmic tail. The DNA vaccine pVAX-S1-TM encodes the S1 subunit of the spike protein (S1; aa 1−661) anchored to the plasma membrane through the transmembrane region (TM). The indicated mutations of Alpha and Delta SARS-CoV-2 variants were sequentially inserted into the S1-TM plasmid, according to a site-directed plasmid mutagenesis protocol. (B) *In silico* three-dimensional (3D) structure of S1-TM spike protein. (Left panel) 3D model of the selected S1-TM spike protein in its trimeric association (gold ribbons), superimposed with trimeric model of full SARS-CoV-2 spike protein in its closed state (pdb code 6vxx; blue ribbons); (middle panel) 3D model of the selected S1-TM spike protein in its trimeric association (coral ribbons), superimposed with trimeric model of full SARS-CoV-2 spike protein in its closed state (pdb code 6vxx; tan ribbons) and the Fab fragments of two neutralizing antibodies targeting RBD domain (6xdg pdb code); (right panel) same as above but with RBD highlighted. The 3D dimensional structure of the S1-TM portion of S-protein was modeled using the Iterative Threading ASSEmbly Refinement (I-TASSER) approach.[20] (C) Representative confocal microscopy images of HEK-293 cells transiently transfected with pVAX-S1-TM-D614G DNA vaccine. Profile of the fluorescence intensity of stained HEK-293 cells expressing SARS-CoV-2 spike protein (green line) and labeled for DAPI (blue line), taken along the white arrows. For imaging, an inverted Zeiss LSM 800 confocal microscope (Jena, Germany) was used. Objective lens 63X/NA1.4; excitation light 405 and 488 nm. Scale bar = 10 μm.

BNT162b2/Comirnaty by BioNTech/Pfizer, have been successfully used for the induction of both humoral and cell-mediated immune responses.[6,7] Despite this, DNA vaccines display additional beneficial features. Indeed, DNA vaccines are more stable, less expensive, faster, and easier to produce than mRNA vaccines.[8] They can be quickly and easily modified and adapted in response to new variants. Moreover, thanks to their lower cost of production and high stability, they potentially might permit achieving global immunization. ZyCoV-D, a DNA vaccine developed against SARS-CoV-2 by Zydus Cadila, has demonstrated full protection against severe disease and death while remaining safe and stable at room temperature.[9] ZyCoV-D approval has been a significant milestone for DNA vaccines, and it represents a catalyst for the development of other DNA-based vaccines.[10,11] Although both electroporation and gene gun are leading methods of DNA vaccine delivery and represent an effective way to increase the DNA vaccine immunogenicity, results emerging from the growing number of clinical trials in humans underline the strong potential of electroporation for DNA vaccination, which combines both efficacy and safety.[12,13] Electroporation, by applying short electrical pulses, induces transient permeability of biological membranes, enhances DNA transfection, and increases the transgene expression by 10- to 1000-fold. Moreover, electroporation stimulates prevalently a Th1-type immune response, required for host defense against intracellular viral pathogens, while gene gun predominantly induces a Th2-type response.[14] Here, we propose a vaccine strategy based on electroporated chimeric DNA vaccines encoding spike antigen-bearing key mutations from different SARS-CoV-2 variants of concern. Since aging is a prominent risk factor for severe disease from COVID-19 and suboptimal vaccine responses, mainly due to age-related decline of immune function, we tested the immunogenicity of our prototype vaccines not only in young but also in aged C57BL/6 mice. INDUK displayed safety and immunogenic properties even in older animals, opening the way for the development of chimeric vaccines potentially able to protect against present and future SARS-CoV-2 variants.

RESULTS

Construction and In Vitro Validation of pVAX-S1-TM-D614G and INDUK DNA Vaccines. Over the course of the past three years, the emergence of SARS-CoV-2 variants, such as Alpha (B.1.1.7), Beta (B.1.351), Gamma (P.1), Delta (B.1.617), and the fast-spreading Omicron (B.1.1.529), with

https://doi.org/10.1021/acsomega.4c03285
ACS Omega 2024, 9, 34624−34635

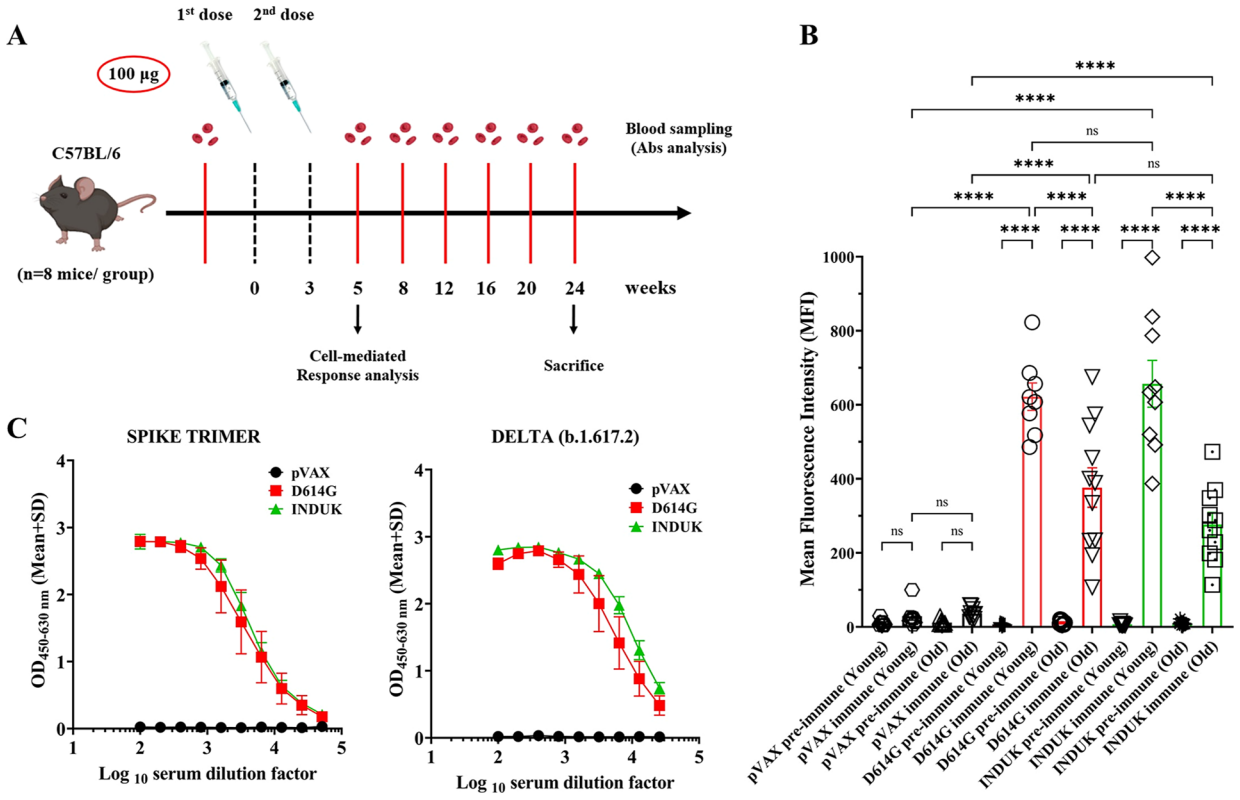

Figure 2. Antibody responses to pVAX-S1-TM-D614G (D614G) (red) and pVAX-S1-TM-INDUK (INDUK) (green) in young and old C57BL/6 mice. (A) Vaccination regimen. pVAX-S1-TM-D614G and pVAX-S1-TM-INDUK vaccines were administered by intramuscular injection (i.m.) followed by electroporation in both young and aged C57BL/6 mice (n = 8 mice/group). Mice underwent a 3-week interval between two consecutive DNA vaccine doses. Two weeks after the last vaccination and once a month for 6 months, blood was harvested for antibody screening. (B) Flow cytometry analysis of the antibody responses elicited in young and old C57BL/6 mice. Bars, Mean ± SEM * $p < 0.05$; ** $p < 0.01$; *** $p < 0.001$; **** $p < 0.0001$; Two-way ANOVA followed by Tukey's multiple comparisons test. (C) Anti-SARS-CoV-2 IgG binding to Spike trimer (left panel) or Delta variant (B.1.617.2) trimer (right panel), in gradient dilutions of sera from immunized mice.

multiple substitutions in the spike protein, has challenged the effectiveness of vaccines available on the market. Thus, we generated chimeric DNA vaccines by sequentially introducing key mutations of selected variants into the spike sequence as a strategy in response to SARS-CoV-2 variants of concern. In particular, two DNA vaccines were constructed, pVAX-S1-TM-D614G and pVAX-S1-TM-INDUK (INDUK), which is a chimeric DNA plasmid encoding the S1 subunit including a combination of key mutations of Alpha and Delta variants (Figure 1A). For this purpose, pVAX-S1-TM, codifying for the S1 subunit (S1; aa 1−661) of the SARS-CoV-2 spike protein in fusion with the transmembrane region (TM), was first generated using pcDNA3.1-SARS2-Spike plasmid (Addgene) as a template and pVAX1 as backbone. Indeed, according to an *in silico* analysis, the transmembrane region associated with the S1 spike subunit permits the trimerization of the antigen, reproducing the conformation of the native Spike protein exposed as a trimer on the surface of the virus. The overall structure was stable and associated in close conformation to the complete SARS-CoV-2 protein in the closed state. Thus, the exposed epitopes on the RBD of the S1-TM antigen can be potentially recognized by neutralizing antibodies (Figure 1B; supplementary Figure S1). Then, the dominant D614G substitution was introduced by a PCR-based site-directed plasmid mutagenesis protocol, as described in the Methods section, to obtain pVAX-S1-TM-D614G (the nucleotide sequence encoding for S1-TM-D614G and its amino acid sequence are available as Supplementary data). The D614G mutation is present in all significant variants of the SARS-CoV-2 virus and confers higher infectivity and transmissibility.[15,16] The chimeric DNA vaccine INDUK was generated by the insertion of additional key mutations from Delta (E484Q and L452R) and Alpha (N501Y and A570D) variants (the nucleotide sequence encoding for INDUK and its amino acid sequence are available as Supplementary data). It is known that N501Y results in an increased binding affinity of the spike protein to the ACE2 receptor enhancing viral attachment to the host cells,[17] A570D plays a key role in modulating the RBD conformational switching in response to host infection,[18] while the other two RBD mutations, E484Q and L452R, reduce binding properties to selected monoclonal antibodies (mAbs) and potentially affect their neutralization capacity.[19] The antigen expression and its proper localization on the plasma membrane were verified in vitro by immunofluorescence assay in HEK-293 cells, transiently transfected with both pVAX-S1-TM-D614G and INDUK (supplementary Figure S2). Confocal microscopy analysis was also performed to further confirm the expression of the S1 spike antigen on the plasma membrane of pVAX-S1-TM-D614G transfected HEK-293 cells (Figure 1C).

Immunogenicity of pVAX-S1-TM-D614G and INDUK DNA Vaccines in C57BL/6 Young and Aged Mice. Aging often results in a marked reduction in immune protection against infection in the elderly, and it is known that SARS-CoV-2 infection leads to higher mortality rates in aged individuals than in younger ones.[21] This decline in immune

https://doi.org/10.1021/acsomega.4c03285
ACS Omega 2024, 9, 34624−34635

function (immunosenescence) might also limit the effectiveness of vaccination in older adults. Thus, the immunogenicity of pVAX-S1-TM-D614G and INDUK was tested not only in young but also in aged mice, as a preclinical model for elderly humans. In particular, two doses of pVAX-S1-TM-D614G and INDUK (100 μg of naked plasmid DNA/mouse), or empty pVAX vector as control, were administered at 21-day intervals, via intramuscular injection followed by electroporation, in young/adults (11 weeks of age) and aged (20 months of age) C57BL/6 mice. Blood samples were collected the day before the first vaccination, 2 weeks after the second vaccination, and once a month for a total period of 6 months, to measure the antibody response and its duration (Figure 2A). The presence of antispike antibodies in the sera of immunized mice was assessed by flow cytometry using HEK-293 cells ectopically expressing SARS-CoV-2-Spike protein as targeted cells. The antispike antibody titer, measured 2 weeks after the second dose (sera collection date: March 23, 2022), was significantly higher in mice vaccinated with pVAX-S1-TM-D614G and INDUK with respect to the pVAX control group, although a wide variation between individuals was observed, especially in the old mice group. Thus, even if the elicited level of antibody was lower in old mice with respect to the young animals, pVAX-S1-TM-D614G and INDUK were immunogenic also in aged individuals (Figure 2B). The ability of the antibodies induced by vaccination with pVAX-S1-TM-D614G and INDUK to recognize the target Spike protein as a trimer was assessed using a commercial ELISA kit, which provides rapid detection of anti-SARS-CoV-2 antibodies in mouse serum by SARS-CoV-2 Spike trimer. The obtained data confirmed the *in silico* prediction of the antigen conformation (Figure 2C, left panel). Moreover, to verify the ability of vaccine-induced antibodies to bind specifically the Delta variant Spike trimer, anti-SARS-CoV-2 (B.1.617.2) IgG antibodies in the serum of vaccinated mice were measured. INDUK appeared to induce antibodies more specific for the Delta variant compared with pVAX-S1-TM-D614G (Figure 2C, right panel), although the difference between the two curves is not statistically significant.

To determine if the humoral immune response included the generation of neutralizing antibodies, serum samples obtained after DNA immunization were analyzed by an ACE2:SARS-CoV-2 spike S1 inhibitor screening assay, designed for screening the capacity of antibodies to block the interaction between the viral spike S1 protein and the ACE2 receptor. As shown in Figure 3, both pVAX-S1-TM-D614G (D614G) and pVAX-S1-TM-INDUK (INDUK) were able to induce neutralizing antibodies in C57BL/6 mice.

Unfortunately, flow cytometry analysis showed a rapid decline in the antibody levels. Only in young mice vaccinated with INDUK, a low but statistically significant level of anti-Spike antibodies persisted until 3 months after the second vaccination (Figure 4A). Both DNA vaccines were unable to elicit a durable antibody response in aged mice (Figure 4B), in which the antibody levels dropped within two months from the last vaccination.

To overcome waning immunity, an additional third dose of pVAX-S1-TM-D614G and INDUK DNA vaccines (booster) was administered to both young and old mice, who had already completed the vaccination cycle by receiving a second dose six months earlier. Blood was collected from immunized mice 2 weeks later to assess the ability of the booster dose to improve the antibody response (Figure 5A). Flow cytometry results showed that booster doses of pVAX-S1-TM-D614G and

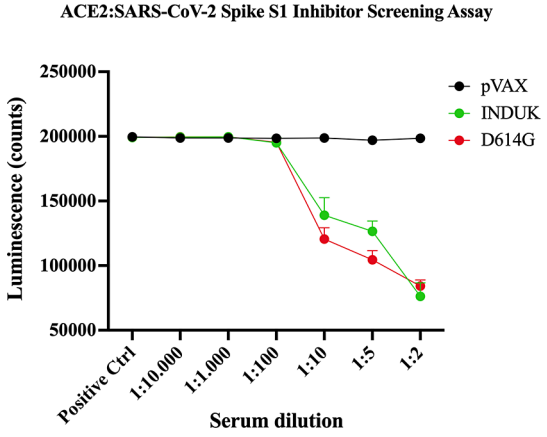

Figure 3. Analysis of functional humoral immune responses induced by the SARS-Cov2 vaccines. The inhibition of the interaction between the spike protein S1 and the human angiotensin-converting enzyme 2 (ACE2) receptor by anti-SARS-CoV-2 antibodies elicited by vaccination was determined based on chemiluminescence measurements as described in Methods section. Sera from young C57BL/6 mice vaccinated with pVAX-S1-TM-D614G (red) or pVAX-S1-TM-INDUK (green) or with empty pVAX (black) were tested at the indicated dilutions (n = 3).

INDUK DNA vaccines significantly increased the magnitude of antispike antibody titers in both young and aged mice (Figure 5B,C), suggesting that our vaccines can provide long-lasting immunity if the vaccination schedule is optimized. Of note, 26-month-old mice displayed a noninferior spike-specific antibody response compared to younger mice after receiving a booster dose.

To evaluate the cellular responses, we collected spleen tissues from vaccinated and controll young and old C57BL/6 mice 2 weeks after the second dose. The splenocytes were then stimulated with spike peptide of SARS-CoV-2, and T cells were analyzed for the production of IFN-γ or tumor necrosis factor-α (TNF-α), which are cytokines involved in T-cell differentiation and proliferation. FlowSight analysis demonstrated that vaccination with INDUK induced an increase in the percentage of IFN-γ producing T lymphocytes in immunized mice, although it was statistically significant only in young animals (Figure 5A), as well as an increase in the percentage of TNF-α-producing T lymphocytes in both young and aged vaccinated mice (Figure 6B). Furthermore, following INDUK and D614G vaccination, older mice exhibited a reduced percentage of T lymphocytes producing IFN-γ and TNF-α in comparison with their younger counterparts (Figure 6A, B).

No signs of toxicity were observed in the vaccinated mice. In particular, autoptic examination of old mice performed at the end of the experiment confirmed that our DNA vaccines did not cause any organ damage.

DISCUSSION

Immunosenescence is the age-related transformation of the immune system, marked by reduced innate and adaptive immune functions.[22,23] Continuous exposure to antigens over a lifetime intensifies this decline, leading to a chronic, low-level inflammation known as "inflammaging," which subsequently compromises immune function.[24−26] This complex interplay significantly heightens susceptibility to infectious diseases such as COVID-19 infection. Vaccination has emerged as a crucial tool in protecting older adults against severe COVID-19

https://doi.org/10.1021/acsomega.4c03285
ACS Omega 2024, 9, 34624−34635

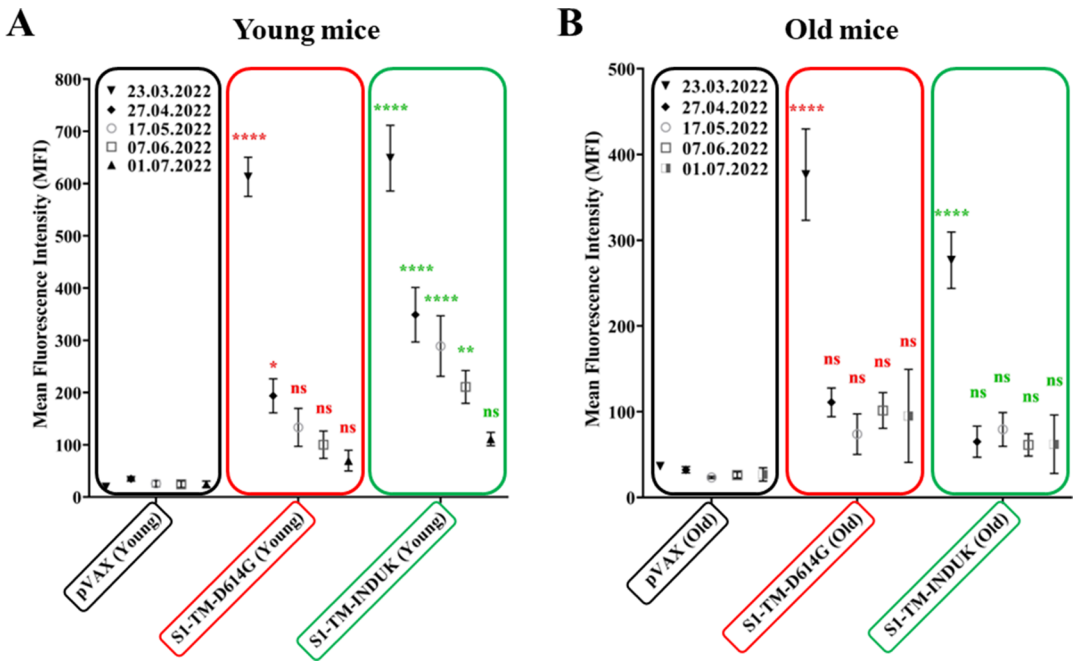

Figure 4. Postvaccination antispike antibody persistency in both young (A) and aged (B) C57BL/6 mice immunized with pVAX-S1-TM-D614G (red) or pVAX-S1-TM-INDUK (green) vaccines or empty pVAX (black) as a control. Antibody levels in the sera of immunized mice were evaluated via flow cytometry on HEK-293 cells transfected with pcDNA3.1-SARS2-Spike. The legends indicate the dates of sera collection. Values are mean ± SEM * $p < 0.05$; ** $p < 0.01$; *** $p < 0.001$; **** $p < 0.0001$; Two-way ANOVA followed by Tukey's multiple comparisons test.

outcomes. While currently available COVID-19 vaccines have demonstrated strong efficacy against the original SARS-CoV-2 strain, their effectiveness has waned against emerging variants, posing a persistent threat of reduced immunity, particularly among older individuals. The two most frequently used SARS-CoV-2 vaccines, mRNA-1273/SpikeVax by Moderna and BNT162b2/Comirnaty by BioNTech/Pfizer, are mRNA vaccines that encode a membrane-anchored SARS-CoV-2 full-length spike protein, stabilized in the prefusion state by adding two proline mutations in the C-terminal S2 fusion domain, in order to reproduce the structure of functional SARS-CoV-2 spike proteins on intact virions, and thus to improve the neutralizing antibody response.[27,28] Indeed, the spike is a large, trimeric glycoprotein that mediates both binding to a host cell receptor, the angiotensin-converting 2 (ACE2) protein, and the fusion of virus and host cell membranes. SARS-CoV-2 spike protein is intrinsically unstable: in the "closed" prefusion state, all three RBDs of the spike trimer are packed tightly together and cannot bind ACE2, while a transition to an "open" spike conformation is required for engagement with the ACE2 protein and successful viral infection of the host cell.[29] Thus, it is crucial for an effective vaccine to generate a spike protein in the native prefusion trimer conformation as a target antigen to train the immune system to recognize the virus before its entry into the host cell. In our study, we assessed the immunogenicity of two DNA vaccines against SARS-CoV-2 variants, pVAX-S1-TM-D614G and INDUK, encoding the S1 spike subunit in fusion with the transmembrane (TM) region. The S1 region of the spike protein was selected since it includes the RBD and the major antigenic sites, while the TM domain was chosen as it is reported to be sufficient to induce the native trimeric structure of spike protein and thus to ensure the relevant antigenic conformation.[30] *In silico* analysis confirmed that the TM region associated with the S1 spike subunit allows the trimerization of the antigen, reproducing the native closed trimer conformation of the spike protein exposed on the surface of the virus. Thus, the overall structure of S1-TM is stable and potentially recognized by neutralizing antibodies. pVAX-S1-TM-D614G includes the dominant D614G substitution, while pVAX-S1-TM-INDUK (INDUK) includes two additional key mutations from Delta (E484Q and L452R) and two from Alpha (N501Y and A570D) variants. When delivered by electroporation in young and aged mice, pVAX-S1-TM-D614G and INDUK were able to trigger a significant antispike antibody response, including neutralizing antibodies, although INDUK elicited a more persistent antibody level with respect to pVAX-S1-TM-D614G in young animals. Superimposition of S1-TM and INDUK trimers, obtained by *in silico* analysis, showed that residue 484, which is directly involved in interactions with the fragment antigen-binding region (Fab region) of an antibody, is differently positioned in the two S1-TM and INDUK trimers (Supplementary Figure S3). This different conformation can account for a different antigenic activity of INDUK and suggests that the mutations inserted in INDUK lead to stabilizing amino acid changes that might improve the antibody response.[31] However, antibody titer induced by both pVAX-S1-TM-D614G and INDUK declined within 6 months after the second dose in all immunized mice, especially in aged mice, in agreement with previous studies reporting that neutralizing antibody responses, raised by mRNA COVID-19 vaccines, decay with a half-life of 69−173 days.[32] Nevertheless, a third booster dose, given at 6 months from the last vaccination, was able to efficiently recall immune memory and reverse anti-SARS-CoV-2 antibody waning even in aged animals. When cellular responses were analyzed, INDUK appeared to be the most immunogenic vaccine, even in the old mice group. However, INDUK and pVAX-S1-TM-D614G elicited fewer T lymphocytes capable of producing IFN-γ and TNF-α in aged mice compared with those in young animals.

https://doi.org/10.1021/acsomega.4c03285
ACS Omega 2024, 9, 34624−34635

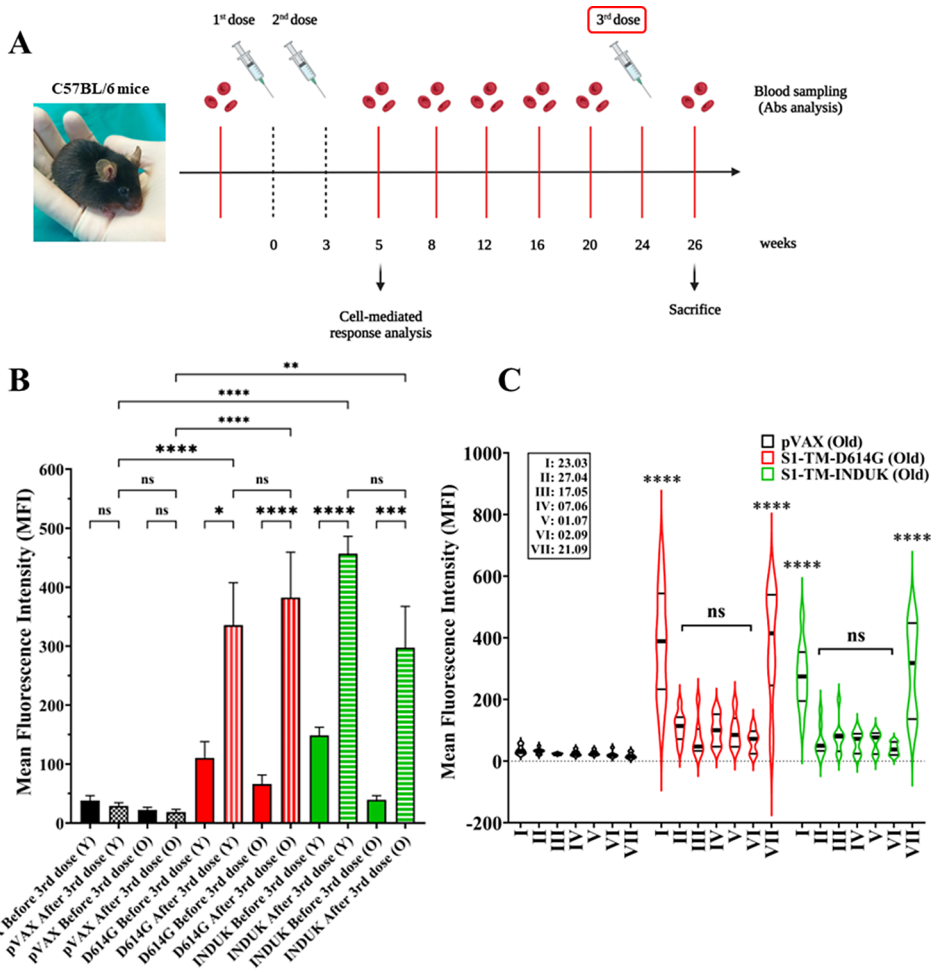

Figure 5. Booster doses increased the magnitude of the antibody titers. (A) Vaccination regimen. pVAX-S1-TM-D614G and pVAX-S1-TM-INDUK vaccines were administered by intramuscular injection (i.m.) followed by electroporation in both young and aged C57BL/6 mice (n = 8 mice/group). Mice underwent a 3-week interval between two consecutive DNA vaccine doses, plus a third booster dose 6 months after the last vaccination, 2 weeks later blood was harvested for antibody screening. (B) Bar graph represents antibody titers in sera of both young (Y) and old (O) mice before and after receiving the third dose of pVAX-S1-TM-D614G (red) or pVAX-S1-TM-INDUK (green) vaccines or empty pVAX (black) as control. (C) Violin plot shows antibody response elicited by two doses of vaccines, its decline during the following six months, and its recall by booster doses in aged mice, measured by flow cytometry. Violin plot, the center thick line represents the median, the thin lines represent the interquartile range, and the violin width indicates kernel density estimates. The legend indicates the numbers of blood sampling and the corresponding dates. Mean ± SEM; *p < 0.05; **p < 0.01; ***p < 0.001; ****p < 0.0001; Two-way ANOVA followed by Tukey's multiple comparisons test.

This may depend on the immunosenescence and the reduced number of CD4-naïve T cells with aging.[33] In fact, recent evidence shows that the depletion of CD4+ T cells led to diminished antibody response and delayed viral clearance, in a murine model of acute SARS-CoV-2 infection.[34] Th1 Cytokines (IFN-γ, TNF-α, and IL-2) produced by Spike-specific T cells are also important regulators of the magnitude, quality, and course of the humoral response.[35] Therefore, the reduced frequency of IFN-γ- and TNF-α-producing T cells in old mice, attributable to the phenomenon of immunosenescence,[36,37] could lead to a more rapid decline in spike-specific antibody response overtime and the need for more frequent booster shots compared with young mice. Although this study has some limitations, including the lack of an evaluation of antibody-dependent cell-mediated cytotoxicity and a deeper characterization of the spike-specific T-cell immunity, such as the measure of the frequency of CD4+ T cells expressing IFN-γ following stimulation with pVAX-S1-TM-D614G and pVAX-S1-TM-INDUK vaccines and the analysis of the balance between Th1 and Th2 responses by means of the ratios between Th1 cytokine concentrations (IFN-γ) and Th2 cytokine concentrations, we can conclude that the chimeric DNA vaccine INDUK is safe and able to elicit functional immune reactions, even in aged mice, when the vaccination schedule is optimized. Future studies aimed at exploring the durability of the cellular immune response elicited by INDUK in aged mice will help to further characterize its immunogenic properties. Another limitation of the present study is that INDUK immunogenicity has been studied only in a mouse model, the C57BL/6 mouse, while further evaluation in other experimental models such as rats and larger animals such as ferrets, which are considered valuable models for SARS-CoV-2 research,[38,39] might be beneficial. Although INDUK includes key mutations from Delta and Alpha SARS-CoV-2 variants that are not anymore circulating, the dominant D614G substitution and N501Y mutation are still present in currently circulating Omicron variants, while residues 484 and 452 are also mutated in some Omicron subvariants. Indeed, the computational

https://doi.org/10.1021/acsomega.4c03285
ACS Omega 2024, 9, 34624−34635

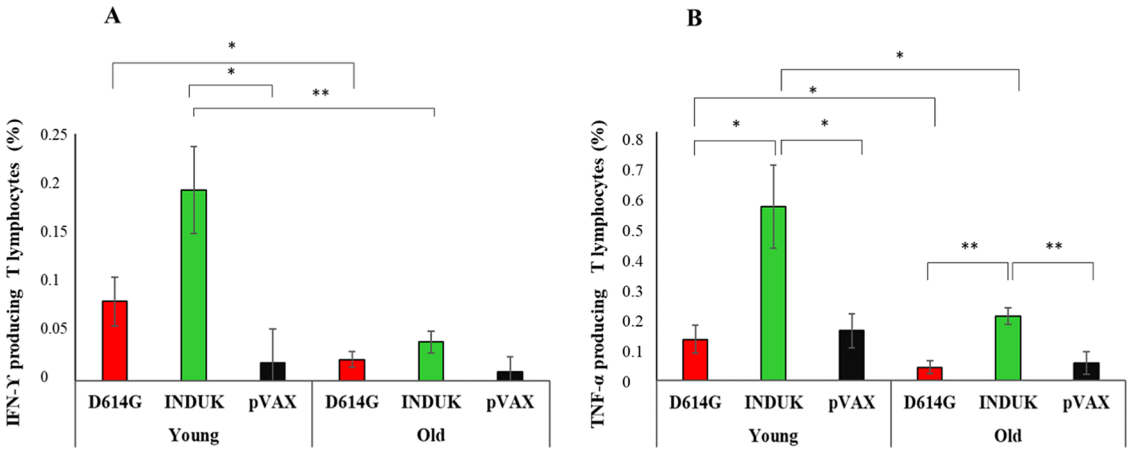

Figure 6. IFN-γ- and TNF-α-producing T lymphocytes in young and aged immunized C57BL/6 mice. INDUK vaccination resulted in an elevation of the proportion of IFN-γ-producing T lymphocytes in immunized mice (A). Vaccination with INDUK induced an increase in the percentage of TNF-α-producing T lymphocytes in both young and aged mice (B). The frequency of splenic IFN-γ- and TNF-α-producing T lymphocytes was lower in aged mice compared with young mice postimmunization. Mean ± SEM; *$p < 0.05$; **$p < 0.001$ by ANOVA analysis.

analysis showed a similar conformation when the two structures (INDUK and Omicron) were superimposed (Figure S3). Recently, the RBD double mutation (L452R and E484Q) has been associated with weakened neutralizing activity and immune evasion, and thus, it should be taken into consideration for the development of effective vaccines and therapeutic antibodies.[40] Different forms of the S protein, including the full-length S protein, RBD, S1 subunit, and S2 subunit, are currently used in preclinical and clinical trials of DNA vaccines for COVID-19. Nucleocapsid protein is another antigen used in a SARS-CoV-2 candidate DNA vaccine.[13,39] However, to the best of our knowledge, in the landscape of DNA vaccines for COVID-19, the chimeric S1-TM antigenic protein encoded by INDUK can be considered unique. Besides the specific immunogenic characteristics of INDUK, it can be defined as a prototype of a rationally designed chimeric vaccine, which derives from the insertion of a few selected key residues from variants of concern in the RBD region of the conformational stable S1-TM trimer, in order to improve the elicited immune response.[31] DNA vaccines can be easily adapted in response to new variants and are cheaper and more stable than currently approved vaccines; thus, they might represent a promising strategy to achieve global immunization. However, in the application of DNA vaccines, some obstacles may need to be overcome. Indeed, biological barriers (cell membrane, endosomes, and nucleus membrane) and low antigen expression may lead to low immunogenicity of DNA vaccines.[13] Improving DNA plasmid delivery and antigen expression may improve the performance of DNA vaccines. Thus, the next challenge for widespread use of DNA vaccines will be their encapsulation in optimized lipid nanoparticles to enhance transfection efficiency and facilitate their administration.[41−43]

METHODS

In Silico Analysis. The 3D dimensional structures of the S1-TM portion of spike SARS-CoV-2 protein and the INDUK variant were modeled using the Iterative Threading ASSEmbly Refinement (I-TASSER) approach.[17] Their trimeric association was reconstructed using the trimeric assembly of spike SARS-CoV-2 protein (6vxx pdb code). Both monomeric and trimeric macromolecular structures have been minimized with 10,000 steepest descent cycles followed by 5000 conjugate gradient steps, obtaining a convergence of maximum force to energy threshold of 1000 kJ/mol nm^2, using CHARMM36m force field within GROMACS 2020.6 software. In order to assess the conformational and association stability, the trimer underwent 100 ns MD simulation using Periodic Boundary Conditions (PBC) in an explicit TIP3P water solvent and NPT ensemble.

Construction of pVAX-S1-TM-D614G and pVAX-S1-TM-INDUK DNA Vaccines. The sequences encoding the S1 and TM regions of the SARS-CoV-2 spike protein were sequentially cloned into the pVAX vector (Invitrogen, Carlsbad, CA), using *NheI/EcoRI* and *Eco*RI/*XhoI* restriction enzymes, respectively. S1 (amino acids 1 to 661) and TM sequences were amplified using pcDNA3.1-SARS2-Spike vector as template (Addgene plasmid # 145032; http://n2t.net/addgene:145032; RRID:Addgene_145032)[44] and the following primers: Forward primer SPIKE-*NheI*: 5′-ACT CAC TAT AGG GAG ACC CAA GCT G-3′; Reverse primer SPIKE-*Eco*RI): 5′-GCG CGA ATT CGT AGG AAT TGT TCA CGT GCT CA-3′. Forward primer TM-*Eco*RI: 5′-GCG CGA ATT CTG GTA CAT CTG GCT GGG CTT C-3′; Reverse primer TM-*XhoI)*: 5′-CCG GCT CGA GCT AAG CGG GAG CGA CCT GGG A-3′. In the reverse primer used for the TM amplification, between the restriction site and the hybridization sequence, a stop codon (underlined) was inserted. The sequence of pVAX-S1-TM was analyzed (BMR Genomics, Padova). To obtain the pVAX-S1-TM-D614G and pVAX-S1-TM-INDUK (INDUK) DNA vaccines, selected mutations were inserted into pVAX-S1-TM using a one-step PCR-based multiple site-directed plasmid mutagenesis protocol.[45] pVAX-S1-TM-D614G includes the D614G mutation, while INDUK includes the D614G mutation plus two key mutations (A570D and N501Y) from the Alpha (B.1.1.7) lineage (previously known as United Kingdom variant, UK) and two key mutations (E484Q and L452R) from the Delta (B.1.617) lineage (previously known as Indian (IND) variant). These few key mutations were selected because they confer higher infectivity and transmissibility to the SARS-CoV-2 virus: the D614G is a dominant substitution present in all SARS-CoV-2 variants; although this mutation is outside of the RBD in the S1 subunit of the spike, it facilitates rapid viral

https://doi.org/10.1021/acsomega.4c03285
ACS Omega 2024, 9, 34624−34635

Table 1. Primers Used in the Mutagenesis Protocol

primers	sequences	Tm_{pp}[a] (°C)	Tm_{no}[b] (°C)
D614G Forw	5′CTGTACCAGGGCGTGAATTGCACCGAGGTGCCAGTGGCTATCCAC 3′	56 °C	65 °C
D614G Rew	5′CAATTCACGCCCTGGTACAGCACGGCCACCTGGTTGCTGGTATTG 3′	56 °C	64.5 °C
N501Y Forw	5′CCAGCCAACCTACGGAGTGGGATACCAGCCATACAGGGTGGTGGT 3′	61 °C	62.2 °C
N501Y Rew	5′CCACTCCGTAGGTTGGCTGGAAGCCGTAGCTCTGCAGGGGGAAGT 3′	59.6 °C	65.8 °C
A570D Forw	5′AAGGGACATCGATGATACCACCGACGCCGTGCGCGACCCACAGAC 3′	52.7 °C	71.8 °C
A570D Rew	5′TGGTATCATCGATGTCCCTTCCGAACTGCTGGAATGGCAGGAACT 3′	52.7 °C	63.5 °C
L452R Forw	5′ACAATTACCGGTACCGCCTGTTCCGCAAGTCCAATCTGAAGCCAT 3′	57.2 °C	61.3 °C
L452R Rew	5′CAGGCGGTACCGGTAATTGTAGTTGCCGCCCACTTTGCTATCCAG 3′	57.2 °C	63.8 °C
E484Q Forw	5′AATGGAGTGCAGGGCTTCAACTGCTACTTCCCCCTGCAGAGCTAC 3′	56.9 °C	62.7 °C
E484Q Rew	5′TTGAAGCCCTGCACTCCATTGCATGGGGTGCTTCCAGCCTGGTAG 3′	56.9 °C	65.6 °C

[a]Tm of the nonoverlapping sequences (Tm_{no}); [b]Tm of the complementary sequences (Tm_{pp}).

spread. The other four mutations are located inside the RBD region; they result in an increased binding affinity of the spike protein to the ACE2 receptor and are associated with virus immune evasion.[15−19]

Primers and reaction conditions used for PCR-based mutagenesis are listed in Table 1.

After *DpnI* restriction enzyme digestion, the newly synthesized PCR products were transformed into *Escherichia coli* cells. Both pVAX-S1-TM-D614G and INDUK were sequenced by BMR Genomics (Padova).

Cell Culture. Human embryonic kidney-293 (HEK-293) cells were obtained from American Type Culture Collection (ATCC, Rockville, MD, USA) and cultured in Dulbecco's Modified Essential Medium (DMEM, Gibco, Life Technologies, Carlsbad, CA, USA) supplemented with 10% fetal bovine serum (FBS, Gibco, Life Technologies) and 1% penicillin−streptomycin (Gibco, Life Technologies). Cells were cultured at 37 °C under a humidified atmosphere with 5% CO_2.

Immunofluorescence Analysis for In Vitro Validation of Candidate DNA Vaccines. HEK-293 cells were plated in a 24-well plate (2×10^5 cells/well). One day after plating, 70−90% of confluent cells were transiently transfected with vaccine candidates (pVAX-S1-TM-D614G and INDUK) or with pVAX and pcDNA3.1-SARS2-SPIKE (Addgene), used as negative and positive controls, respectively, using Lipofectamine 3000, according to the manufacturer's instructions. Forty-eight hours after transfection, cells were fixed for 10 min with phosphate-buffered saline (PBS)-4% paraformaldehyde (Sigma, St. Louis, MO). After incubation in blocking buffer (PBS-10% bovine serum albumin (BSA; Sigma, Milan, Italy) for 20 min, cells were incubated for 1 h at 37 °C with the primary antibody SARS-CoV-2 (COVID-19) Spike S1 antibody [HL134] (GTX635671) (antirabbit, 1:100). After washing, cells were incubated with Goat antirabbit IgG Alexa Fluor 488 secondary antibody (Invitrogen Molecular Probes, Eugene, OR, USA) diluted at 1:200 for 1 h at 37 °C. DAPI staining (dilution factor 1:1000) was performed incubating cells for 10 min. To observe the antigen expression, cells were examined under a Fluorescence Microscope (Carl Zeiss GmbH, Germany) or a Zeiss LSM 800 confocal microscope (Jena, Germany) with a 63× 1.4 NA oil immersion objective at 405 and 488 nm excitation. For confocal images, Z-stack acquisitions were performed using a step size of 0.6 μm. The XZ, YZ projections, and intensity plot profile were performed using Fiji, and plotted by Origin (OriginLab Corporation, Origin 2019b).

Mice. The C57BL/6 mice were housed at a controlled temperature (20 °C) and circadian cycle (12 h light/12 h dark), in an SPF zootechnical facility (free from specific pathogens) approved with ministerial authorization no. 11/2015-UT of 09/14/2015 (2010/63/EU). The animals were fed on a chow diet (Mucedola 4RF25 autoclavable) and tap water *ad libitum*. Mice were treated in accordance with the UK Animals (Scientific Procedures) Act, 1986 and associated guidelines, EU Directive 2010/63/EU for animal experiments, and the 3Rs principles. All animal experiments were authorized by the Italian Ministry of Health (#708/2021-PR) and by the Animal Research Committee (OPBA) of the National Institute of Health and Science on Aging (INRCA − Istituto Nazionale di Riposo e Cura per Anziani), Ancona (Italy).

SARS-CoV-2 DNA Vaccine Preparation. *E. coli* strain DH5α was transformed with pVAX-S1-TM-D614G and INDUK DNA plasmids and then grown in Luria−Bertani medium with 50 μg/mL kanamycin (Sigma-Aldrich). Large-scale preparation of the plasmids was carried out by alkaline lysis using Endofree Qiagen Plasmid-Giga kit (Qiagen, Chatsworth, CA, USA) according to the manufacturer's instructions. Subsequently, DNA was resuspended in saline (0.9% sodium chloride (NaCl) solution) and stored in aliquots at −20 °C, after concentration determination using a NanoDrop spectrophotometer (Thermo Scientific). Each aliquot contained 100 μL of pVAX-S1-TM-D614G or INDUK DNA plasmids, at a concentration of 1 mg/mL.

Mice Immunization with SARS-CoV-2 DNA Vaccines. Young/adults (11 weeks of age) and aged (20 months of age) C57BL/6 male mice were immunized by two intramuscular (i.m.) injections into the tibial muscle of 50 μg of the plasmids in 50 μL of 0.9% NaCl, followed by electroporation using T820 electroporator (BTX), 2 square-ware 25 ms, 375 V/cm pulse, as previously reported.[46−48] Thus, mice underwent two DNA vaccine boosts at three-week intervals with 100 μg of pVAX-S1-TM-D614G or INDUK DNA vaccines or pVAX empty control vector. Electroporation was performed under anesthesia (mixture of oxygen and nitrous oxide nitrogen and isoflurane at 4% in spontaneous breathing during induction then at 1−0.8% in maintenance in mask). Eventually, a third booster dose was administered six months after the last vaccination. Blood was collected from the retro-orbital plexus under anesthesia, and the maximum volume of each blood sample was 100 μL/mouse, in compliance with regulations and guidelines for laboratory animals in research as well as with ethical standards. To collect serum, whole blood samples were left to clot at room temperature for 30 min. Serum separation was accomplished by centrifugation at 6000 rpm at 4 °C.

Analysis of Antibody Response by Flow Cytometry. Sera from immunized mice were analyzed by flow cytometry

https://doi.org/10.1021/acsomega.4c03285
ACS Omega 2024, 9, 34624−34635

(BD FACSCalibur), using HEK-293 cells transfected with pcDNA3.1-SARS2-Spike vector (Plasmid#145032 from Addgene) as targeted cells, and nontransfected HEK-293 cells as negative controls. Briefly, subconfluent cells were detached and dispensed at a density of 10^6 cells/tube. After 3 min centrifugation at 1000 rpm at 4 °C, the obtained cell pellet was resuspended and washed in staining buffer (2% FBS, 0.05% sodium azide-containing 1× PBS). Cells were incubated with sera of immunized mice for 1 h on ice. After three washes, cells were incubated with the goat antimouse IgG Alexa Fluor 488 secondary antibody (Invitrogen Molecular Probes, Eugene, OR) for 1 h on ice. Cells were washed and resuspended in PBS before the analysis was performed using FACS equipped with Cell Quest software (BD Pharmingen, BD Life Sciences, San Jose, CA, USA). FlowJo software (BD Life Sciences, San Jose, CA, USA) was employed for data analysis.

Measurement of Antibody Titers by ELISA. ELISA assays were performed to detect mouse Anti-SARS-CoV-2 antibodies (IgG) in the sera of immunized young animals, using two commercial kits (ACROBiosystems, RAS-T023 and RAS-T070), according to the manufacturer's instructions. The first kit, Mouse Anti-SARS-CoV-2 Antibody IgG Titer Serologic Assay Kit (Spike Trimer), was used to determine the specificity of the binding of anti-SARS-CoV-2 antibodies to Spike trimer; the second kit was used to determine the specificity of the binding of anti-SARS-CoV-2 antibodies to the Delta variant (B.1.617.2) Spike Trimer. In detail, diluted sera were incubated in a precoated SARS-CoV-2 Spike Trimer microplate for 1 h at 37 °C. Then, plates were washed three times with 1× washing buffer and incubated with horseradish peroxidase (HRP)-goat antimouse IgG for 1 h at 37 °C in the dark. After five washes, 100 μL of TMB (3,3′,5,5′-tetramethylbenzidine) substrate solution was added to the wells and incubated at 37 °C for 20 min in the dark. The reaction was stopped with stop solution, and the plates were read at 450 and 630 nm wavelengths using a microplate reader (FLUOstar Omega, BMG Labtech).

ACE2/SARS-CoV-2 Spike Inhibitor Screening Assay. The BPS Bioscience #79936 ACE2/SARS-CoV-2 spike inhibitor screening kit was used, according to the manufacturer's instructions, to test the ability of immune sera to neutralize viral spikes. Briefly, a 96-well nickel-coated plate was coated with an ACE2-His solution and incubated for 60 min before being washed. Then, the plate was incubated with a blocking buffer. Next, serial dilution of the immune sera was added and incubated for 1 h at room temperature with slow shaking. After the incubation, SARS-CoV-2 Spike (S1)-Fc was added to each well except to the blank, and the reaction was incubated with gentle shaking. After incubation with a blocking buffer, an antimouse-Fc-HRP was incubated and a horseradish peroxidase (HRP) substrate was added to the plate to produce chemiluminescence, which then could be measured using a FluoStar Omega microplate reader.

Flow Cytometry for Splenocytes Analysis. Splenocytes (SPC) were isolated 15 days after the second immunization from vaccinated mice and were collected by smashing spleens on a 40 μm pore cell strainer, centrifuging the resulting cells at 300*g*, for 10 min, and incubating them in erythrocyte lysing buffer for 5 min at room temperature, then splenocytes were frozen in FBS/10% dimethyl sulfoxide (DMSO) (Sigma-Aldrich) and cryopreserved in liquid nitrogen for further evaluation by flow cytometry. For in vitro stimulation assays, frozen aliquots were slightly thawed at 37 °C and then quickly transferred in a partially frozen state into 15 mL Falcon tubes. Cell viability assessment was conducted using Trypan blue staining. Afterward, the cells were centrifuged at 300*g* for 5 min in a 5810R centrifuge (Eppendorf). Supernatants were discarded and splenocytes were resuspended in the culture media and plated at 2×10^6 cells per well in 24-well plates, and incubated with 1 μg/mL peptide (S511−518, determined to be the minimal epitope for SARS-CoV2) or $HSVgB_{498-505}$ as negative control[49] and 3 μg/mL brefeldin A overnight at 37 °C. After stimulation, cells were surfaced-stained with FITC antimouse CD3 antibody (1.0 μg/1 × 10^6 cells; 100204 Biolegend) in Cell Staining Buffer (Biolegend). After fixation and permeabilization according to the manufacturer's instructions, cells were washed in Intracellular Staining Perm Wash Buffer (Biolegend) and stained for intracellular cytokines using APC IFNγ (XMG1.2; Tonbo Biosciences) or TNF-α (MP6-XT22; BD Biosciences) (0.5 μg/10^6 cells) diluted in Intracellular Staining Perm Wash Buffer for 20 min in the dark at room temperature. After a final wash, flow cytometry data were acquired on a FlowSight system (Amnis, part of Merck Millipore, Seattle, WA, USA), an advanced imaging flow cytometer that combines features of fluorescence microscopy and flow cytometry. The instrument was operated with 488, 642, and 785 nm lasers at 20, 2, and 5.62 mW. Analysis was performed with the dedicated image analysis software (IDEAS v6.2), which allows advanced quantification of intensity, location, morphology, population statistics, and more, within tens of thousands of cells per sample. To quantify the % of positive cells we used the mean fluorescence intensity collected in Ch02 (band 480−560 nm) and Ch11 (band 640−745 nm) after the selection of focused and single cells following established procedures.[50]

Statistical Analysis. Each experiment was performed at least three times independently. Quantitative data are presented as means ± SEM from three independent experiments. The significance of differences was evaluated with a two-tailed Student's *t* test, or one-way ANOVA. Statistical analysis was carried out with GraphPad Prism 9 software (San Diego, CA, USA). A p value of ≤0.05 was used as the critical level of significance. *P* values are indicated in figure legends.

■ ASSOCIATED CONTENT

Supporting Information

The Supporting Information is available free of charge at https://pubs.acs.org/doi/10.1021/acsomega.4c03285.

Molecular models of the S1-TM (Figure S1) and INDUK (Figure S3) antigens encoded by the pVAX-S1-TM and pVAX-S1-TM-INDUK DNA vaccines, respectively, and their expression in transfected HEK-293 cells (Figure S2); Nucleotide and amino acid sequences of S1-TM-D614G and INDUK are reported (PDF)

■ AUTHOR INFORMATION

Corresponding Authors

Daniela Pozzi − *NanoDelivery Lab, Department of Molecular Medicine, Sapienza University of Rome, 00161 Rome, Italy*; Email: daniela.pozzi@uniroma1.it

Cristina Marchini − *School of Biosciences and Veterinary Medicine, University of Camerino, 62032 Camerino, Italy;*

https://doi.org/10.1021/acsomega.4c03285
ACS Omega 2024, 9, 34624−34635

orcid.org/0000-0001-7692-8428; Phone: +39 0737 403275; Email: cristina.marchini@unicam.it

Authors

Lishan Cui − *School of Biosciences and Veterinary Medicine, University of Camerino, 62032 Camerino, Italy;* orcid.org/0000-0001-7647-1376

Junbiao Wang − *School of Biosciences and Veterinary Medicine, University of Camerino, 62032 Camerino, Italy*

Fiorenza Orlando − *Experimental Animal Models for Aging Unit, Scientific Technological Area, IRRCS INRCA, 60100 Ancona, Italy*

Robertina Giacconi − *Advanced Technology Center for Aging Research, IRCCS INRCA, 60100 Ancona, Italy*

Marco Malavolta − *Advanced Technology Center for Aging Research, IRCCS INRCA, 60100 Ancona, Italy*

Beatrice Bartozzi − *Advanced Technology Center for Aging Research, IRCCS INRCA, 60100 Ancona, Italy*

Roberta Galeazzi − *Department of Life and Environmental Sciences, Marche Polytechnic University, 60131 Ancona, Italy*

Giorgia Giorgini − *Department of Life and Environmental Sciences, Marche Polytechnic University, 60131 Ancona, Italy*

Luca Pesce − *NEST Laboratory, Scuola Normale Superiore, 56127 Pisa, Italy*

Francesco Cardarelli − *NEST Laboratory, Scuola Normale Superiore, 56127 Pisa, Italy;* orcid.org/0000-0003-3049-5940

Erica Quagliarini − *NanoDelivery Lab, Department of Molecular Medicine, Sapienza University of Rome, 00161 Rome, Italy*

Serena Renzi − *NanoDelivery Lab, Department of Molecular Medicine, Sapienza University of Rome, 00161 Rome, Italy*

Siyao Xiao − *NanoDelivery Lab, Department of Molecular Medicine, Sapienza University of Rome, 00161 Rome, Italy*

Mauro Provinciali − *Experimental Animal Models for Aging Unit, Scientific Technological Area, IRRCS INRCA, 60100 Ancona, Italy*

Giulio Caracciolo − *NanoDelivery Lab, Department of Molecular Medicine, Sapienza University of Rome, 00161 Rome, Italy;* orcid.org/0000-0002-8636-4475

Augusto Amici − *School of Biosciences and Veterinary Medicine, University of Camerino, 62032 Camerino, Italy*

Complete contact information is available at: https://pubs.acs.org/10.1021/acsomega.4c03285

Author Contributions

L.C. and J.W. contributed equally as the first authors. C.M. and A.A. contributed equally as the last authors. Conceptualization, L.C., J.W., C.M., and A.A.; methodology, M.P., A.A.; formal analysis, R.G., L.C., C.M., A.A.; investigation, L.C., J.W., F.O., R.G., B.B., M.M., G.G., R.Galeazzi, L.P., F.C., E.Q., S.R., S.X., A.A.; writing-original draft preparation, L.C. and C.M.; writing-review and editing, L.C., C.M., F.C., D.P., M.P., G.C., A.A.; supervision, C.M., and A.A.; project administration, C.M., M.P., G.C. and A.A.; funding acquisition, C.M. and A.A. All authors have read and agreed to the published version of the manuscript.

Notes

The authors declare no competing financial interest.

ACKNOWLEDGMENTS

This project has been supported by Regione Marche (BVI422003).

REFERENCES

(1) Li, Q.; Guan, X.; Wu, P.; Wang, X.; Zhou, L.; Tong, Y.; Ren, R.; Leung, K. S. M.; Lau, E. H. Y.; Wong, J. Y.; Xing, X.; Xiang, N.; Wu, Y.; Li, C.; Chen, Q.; Li, D.; Liu, T.; Zhao, J.; Liu, M.; Tu, W.; Chen, C.; Jin, L.; Yang, R.; Wang, Q.; Zhou, S.; Wang, R.; Liu, H.; Luo, Y.; Liu, Y.; Shao, G.; Li, H.; Tao, Z.; Yang, Y.; Deng, Z.; Liu, B.; Ma, Z.; Zhang, Y.; Shi, G.; Lam, T. T. Y.; Wu, J. T.; Gao, G. F.; Cowling, B. J.; Yang, B.; Leung, G. M.; Feng, Z. Early Transmission Dynamics in Wuhan, China, of Novel Coronavirus-Infected Pneumonia. *N. Engl. J. Med.* **2020**, *382* (13), 1199−1207.

(2) Lai, C. C.; Shih, T. P.; Ko, W. C.; Tang, H. J.; Hsueh, P. R. Severe acute respiratory syndrome coronavirus 2 (SARS-CoV-2) and coronavirus disease-2019 (COVID-19): The epidemic and the challenges. *Int. J. Antimicrob. Agents* **2020**, *55* (3), No. 105924.

(3) Magazine, N.; Zhang, T.; Wu, Y.; Mcgee, M. C.; Veggiani, G.; Huang, W. Mutations and Evolution of the SARS-CoV-2 Spike Protein. *Viruses* **2022**, *14* (3), 640.

(4) Wrapp, D.; Wang, N.; Corbett, K. S.; Goldsmith, J. A.; Hsieh, C. L.; Abiona, O.; Graham, B. S.; McLellan, J. S. Cryo-EM structure of the 2019-nCoV spike in the prefusion conformation. *Science (New York, N.Y.)* **2020**, *367* (6483), 1260−1263.

(5) Huang, Y.; Yang, C.; Xu, X. F.; Xu, W.; Liu, S. W. Structural and functional properties of SARS-CoV-2 spike protein: potential antivirus drug development for COVID-19. *Acta Pharmacol. Sin.* **2020**, *41* (9), 1141−1149.

(6) Baden, L. R.; El sahly, H. M.; Essink, B.; Kotloff, K.; Frey, S.; Novak, R.; Diemert, D.; Spector, S. A.; Rouphael, N.; Creech, C. B.; Mcgettigan, J.; Khetan, S.; Segall, N.; Solis, J.; Brosz, A.; Fierro, C.; Schwartz, H.; Neuzil, K.; Corey, L.; Gilbert, P.; Janes, H.; Follmann, D.; Marovich, M.; Mascola, J.; Polakowski, L.; Ledgerwood, J.; Graham, B. S.; Bennett, H.; Pajon, R.; Knightly, C.; Leav, B.; Deng, W.; Zhou, H.; Han, S.; Ivarsson, M.; Miller, J.; Zaks, T.; COVE Study Group. Efficacy and Safety of the mRNA-1273 SARS-CoV-2 Vaccine. *N. Engl. J. Med.* **2021**, *384* (5), 403−416.

(7) Sahin, U.; Muik, A.; Vogler, I.; Derhovanessian, E.; Kranz, L. M.; Vormehr, M.; Quandt, J.; Bidmon, N.; Ulges, A.; Baum, A.; Pascal, K. E.; Maurus, D.; Brachtendorf, S.; Lörks, V.; Sikorski, J.; Koch, P.; Hilker, R.; Becker, D.; Eller, A. K.; Grützner, J.; Tonigold, M.; Boesler, C.; Rosenbaum, C.; Heesen, L.; Kühnle, M. C.; Poran, A.; Dong, J. Z.; Luxemburger, U.; Kemmer-Brück, A.; Langer, D.; Bexon, M.; Bolte, S.; Palanche, T.; Schultz, A.; Baumann, S.; Mahiny, A. J.; Boros, G.; Reinholz, J.; Szabó, G. T.; Karikó, K.; Shi, P. Y.; Fontes-garfias, C.; Perez, J. L.; Cutler, M.; Cooper, D.; Kyratsous, C. A.; Dormitzer, P. R.; Jansen, K. U.; Türeci, Ö. BNT162b2 vaccine induces neutralizing antibodies and poly-specific T cells in humans. *Nature* **2021**, *595* (7868), 572−577.

(8) Silveira, M. M.; Moreira, G. M. S. G.; Mendonça, M. DNA vaccines against COVID-19: Perspectives and challenges. *Life Sci.* **2021**, *267*, No. 118919.

(9) Khobragade, A.; Bhate, S.; Ramaiah, V.; Deshpande, S.; Giri, K.; Phophle, H.; Supe, P.; Godara, I.; Revanna, R.; Nagarkar, R.; Sanmukhani, J.; Dey, A.; Rajanathan, T. M. C.; Kansagra, K.; Koradia, P. Efficacy, safety, and immunogenicity of the DNA SARS-CoV-2 vaccine (ZyCoV-D): the interim efficacy results of a phase 3, randomised, double-blind, placebo-controlled study in India. *Lancet* **2022**, *399* (10332), 1313−1321.

(10) Sheridan, C. First COVID-19 DNA vaccine approved, others in hot pursuit. *Nat. Biotechnol.* **2021**, *39* (12), 1479−1482.

(11) Mallapaty, S. India's DNA COVID vaccine is a world first - more are coming. *Nature* **2021**, *597* (7875), 161−162.

(12) Lambricht, L.; Lopes, A.; Kos, S.; Sersa, G.; Préat, V.; Vandermeulen, G. Clinical potential of electroporation for gene therapy and DNA vaccine delivery. *Expert Opin Drug Delivery* **2016**, *13* (2), 295−310.

(13) Shafaati, M.; Saidijam, M.; Soleimani, M.; Hazrati, F.; Mirzaei, R.; Amirheidari, B.; Tanzadehpanah, H.; Karampoor, S.; Kazemi, S.; Yavari, B.; Mahaki, H.; Safaei, M.; Rahbarizadeh, F.; Samadi, P.; Ahmadyousefi, Y. A brief review on DNA vaccines in the era of COVID-19. *Future Virol.* **2022**, *17* (1), 49−66.
(14) Wang, S.; Zhang, C.; Zhang, L.; Li, J.; Huang, Z.; Lu, S. The relative immunogenicity of DNA vaccines delivered by the intramuscular needle injection, electroporation and gene gun methods. *Vaccine.* **2008**, *26* (17), 2100−2110.
(15) Korber, B.; Fischer, W. M.; Gnanakaran, S.; Yoon, H.; Theiler, J.; Abfalterer, W.; Hengartner, N.; Giorgi, E. E.; Bhattacharya, T.; Foley, B.; Hastie, K. M.; Parker, M. D.; Partridge, D. G.; Evans, C. M.; Freeman, T. M.; De Silva, T. I.; Sheffield COVID-19 Genomics Group; McDanal, C.; Perez, L. G.; Tang, H.; Moon-Walker, A.; Whelan, S. P.; Labranche, C. C.; Saphire, E. O.; Montefiori, D. C. Tracking Changes in SARS-CoV-2 Spike: Evidence that D614G Increases Infectivity of the COVID-19 Virus. *Cell* **2020**, *182* (4), 812−827.
(16) Plante, J. A.; Liu, Y.; Liu, J.; Xia, H.; Johnson, B. A.; Lokugamage, K. G.; Zhang, X.; Muruato, A. E.; Zou, J.; Fontes-Garfias, C. R.; Mirchandani, D.; Scharton, D.; Bilello, J. P.; Ku, Z.; An, Z.; Kalveram, B.; Freiberg, A. N.; Menachery, V. D.; Xie, X.; Plante, K. S.; Weaver, S. C.; Shi, P. Y. Spike mutation D614G alters SARS-CoV-2 fitness. *Nature* **2021**, *592* (7852), 116−121.
(17) Cheng, L.; Song, S.; Zhou, B.; Ge, X.; Yu, J.; Zhang, M.; Ju, B.; Zhang, Z. Impact of the N501Y substitution of SARS-CoV-2 Spike on neutralizing monoclonal antibodies targeting diverse epitopes. *Virol. J.* **2021**, *18* (1), 87.
(18) Yang, T.-J.; Yu, P.-Y.; Chang, Y.-C.; Liang, K.-H.; Tso, H.-C.; Ho, M.-R.; Chen, W. Y.; Lin, H. T.; Wu, H. C.; Hsu, S.-T. D. Effect of SARS-CoV-2 B.1.1.7 mutations on spike protein structure and function. *Nat. Struct. Mol. Biol.* **2021**, *28* (9), 731−739.
(19) Cherian, S.; Potdar, V.; Jadhav, S.; Yadav, P.; Gupta, N.; Das, M.; Rakshit, P.; Singh, S.; Abraham, P.; Panda, S.; Team, N. SARS-CoV-2 Spike Mutations, L452R, T478K, E484Q and P681R, in the Second Wave of COVID-19 in Maharashtra, India. *Microorganisms* **2021**, *9* (7), 1542.
(20) Harracha, M. F.; Drossel, B. Structure and dynamics of TIP3P, TIP4P, and TIP5P water near smooth and atomistic walls of different hydroaffinity. *J. Chem. Phys.* **2014**, *140* (17), 174501.
(21) Chen, Y.; Klein, S. L.; Garibaldi, B. T.; Li, H.; Wu, C.; Osevala, N. M.; Li, T.; Margolick, J. B.; Pawelec, G.; Leng, S. X. Aging in COVID-19: Vulnerability, immunity and intervention. *Ageing Res. Rev.* **2021**, *65*, No. 101205.
(22) Aw, D.; Silva, A. B.; Palmer, D. B. Immunosenescence: emerging challenges for an ageing population. *Immunology* **2007**, *120* (4), 435−446.
(23) Aiello, A.; Farzaneh, F.; Candore, G.; Caruso, C.; Davinelli, S.; Gambino, C. M.; Ligotti, M. E.; Zareian, N.; Accardi, G. Immunosenescence and its hallmarks: How to oppose aging strategically? A review of potential options for therapeutic intervention. *Front. Immunol.* **2019**, *10*, 2247.
(24) Fulop, T.; Dupuis, G.; Baehl, S.; Le page, A.; Bourgade, K.; Frost, E.; Witkowski, J. M.; Pawelec, G.; Larbi, A.; Cunnane, S. From inflamm-aging to immune-paralysis: A slippery slope during aging for immune-adaptation. *Biogerontology* **2016**, *17*, 147−157.
(25) Fulop, T.; Larbi, A.; Dupuis, G.; Le page, A.; Frost, E. H.; Cohen, A. A.; Witkowski, J. M.; Franceschi, C. Immunosenescence and inflamm-aging as two sides of the same coin: Friends or foes? *Front. Immunol.* **2018**, *8*, 1960.
(26) Fülöp, T.; Dupuis, G.; Witkowski, J. M.; Larbi, A. The role of immunosenescence in the development of age-related diseases. *Rev. Investig. Clin.* **2016**, *68*, 84−91.
(27) Anderson, E. J.; Rouphael, N. G.; Widge, A. T.; Jackson, L. A.; Roberts, P. C.; Makhene, M.; Chappell, J. D.; Denison, M. R.; Stevens, L. J.; Pruijssers, A. J.; McDermott, A. B.; Flach, B.; Lin, B. C.; Doria-Rose, N. A.; O'Dell, S.; Schmidt, S. D.; Corbett, K. S.; Swanson, P. A., 2nd; Padilla, M.; Neuzil, K. M.; Bennett, H.; Leav, B.; Makowski, M.; Phadke, V. K.; Rostad, C. A.; Ledgerwood, J. E.; Graham, B. S.; Beigel, J. H.; mRNA-1273 Study Group. Safety and Immunogenicity of SARS-CoV-2 mRNA-1273 Vaccine in Older Adults. *N. Engl. J. Med.* **2020**, *383* (25), 2427−2438.
(28) Jackson, L. A.; Anderson, E. J.; Rouphael, N. G.; Roberts, P. C.; Makhene, M.; Coler, R. N.; McCullough, M. P.; Chappell, J. D.; Denison, M. R.; Stevens, L. J.; Pruijssers, A. J.; McDermott, A.; Flach, B.; Doria-Rose, N. A.; Corbett, K. S.; Morabito, K. M.; O'Dell, S.; Schmidt, S. D.; Swanson, P. A., 2nd; Padilla, M.; Mascola, J. R.; Neuzil, K. M.; Bennett, H.; Sun, W.; Peters, E.; Makowski, M.; Albert, J.; Cross, K.; Buchanan, W.; Pikaart-Tautges, R.; Ledgerwood, J. E.; Graham, B. S.; Beigel, J. H.; mRNA-1273 Study Group. An mRNA Vaccine against SARS-CoV-2 - Preliminary Report. *N. Engl. J. Med.* **2020**, *383* (20), 1920−1931.
(29) Hsieh, C. L.; Goldsmith, J. A.; Schaub, J. M.; Divenere, A. M.; Kuo, H. C.; Javanmardi, K.; Le, K. C.; Wrapp, D.; Lee, A. G.; Liu, Y.; Chou, C. W.; Byrne, P. O.; Hjorth, C. K.; Johnson, N. V.; Ludes-meyers, J.; Nguyen, A. W.; Park, J.; Wang, N.; Amengor, D.; Lavinder, J. J.; Ippolito, G. C.; Maynard, J. A.; Finkelstein, I. J.; McLellan, J. S. Structure-based design of prefusion-stabilized SARS-CoV-2 spikes. *Science* **2020**, *369* (6510), 1501−1505.
(30) Azad, T.; Singaravelu, R.; Crupi, M. J. F.; Jamieson, T.; Dave, J.; Brown, E. E. F.; Rezaei, R.; Taha, Z.; Boulton, S.; Martin, N. T.; Surendran, A.; Poutou, J.; Ghahremani, M.; Nouri, K.; Whelan, J. T.; Duong, J.; Tucker, S.; Diallo, J. S.; Bell, J. C.; Nd ilkow, C. S. Implications for SARS-CoV-2 Vaccine Design: Fusion of Spike Glycoprotein Transmembrane Domain to Receptor-Binding Domain Induces Trimerization. *Membranes (Basel)* **2020**, *10* (9), 215.
(31) Dickey, T. H.; Tang, W. K.; Butler, B.; Ouahes, T.; Orr-Gonzalez, S.; Salinas, N. D.; Lambert, L. E.; Tolia, N. H. Design of the SARS-CoV-2 RBD vaccine antigen improves neutralizing antibody response. *Sci. Adv.* **2022**, *8* (37), No. eabq8276.
(32) Doria-Rose, N.; Suthar, M. S.; Makowski, M.; O'Connell, S.; McDermott, A. B.; Flach, B.; Ledgerwood, J. E.; Mascola, J. R.; Graham, B. S.; Lin, B. C.; O'Dell, S.; Schmidt, S. D.; Widge, A. T.; Edara, V. V.; Anderson, E. J.; Lai, L.; Floyd, K.; Rouphael, N. G.; Zarnitsyna, V.; Roberts, P. C.; Makhene, M.; Buchanan, W.; Luke, C. J.; Beigel, J. H.; Jackson, L. A.; Neuzil, K. M.; Bennett, H.; Leav, B.; Albert, J.; Kunwar, P.; mRNA-1273 Study Group. Antibody Persistence through 6 Months after the Second Dose of mRNA-1273 Vaccine for Covid-19. *N. Engl. J. Med.* **2021**, *384* (23), 2259−2261.
(33) Xie, J.; Zhang, J.; Wu, H.; Tang, X.; Liu, J.; Cheng, G.; Li, P. The influences of age on T lymphocyte subsets in C57BL/6 mice. *Saudi J. Biol. Sci.* **2017**, *24* (1), 108−113.
(34) Israelow, B.; Mao, T.; Klein, J.; Song, E.; Menasche, B.; Omer, S. B.; Iwasaki, A. Adaptive immune determinants of viral clearance and protection in mouse models of SARS-CoV-2. *Sci. Immunol.* **2021**, *6* (64), No. eabl4509.
(35) Agrati, C.; Castilletti, C.; Goletti, D.; Meschi, S.; Sacchi, A.; Matusali, G.; Bordoni, V.; Petrone, L.; Lapa, D.; Notari, S.; Vanini, V.; Colavita, F.; Aiello, A.; Agresta, A.; Farroni, C.; Grassi, G.; Leone, S.; Vaia, F.; Capobianchi, M. R.; Ippolito, G.; Puro, V. Coordinate Induction of Humoral and Spike Specific T-Cell Response in a Cohort of Italian Health Care Workers Receiving BNT162b2 mRNA Vaccine. *Microorganisms* **2021**, *9* (6), 1315.
(36) Franceschi, C.; Campisi, J. Chronic inflammation (inflammaging) and its potential contribution to age-associated diseases. *J. Gerontol. Ser. A Biol. Sci. Med. Sci.* **2014**, *69*, S4−S9.
(37) Franceschi, C.; Garagnani, P.; Parini, P.; Giuliani, C.; Santoro, A. Inflammaging: A new immune−metabolic viewpoint for age-related diseases. *Nat. Rev. Endocrinol.* **2018**, *14*, 576−590.
(38) Ciurkiewicz, M.; Armando, F.; Schreiner, T.; De Buhr, N.; Pilchová, V.; Krupp-Buzimikic, V.; Gabriel, G.; Von Köckritz-Blickwede, M.; Baumgärtner, W.; Schulz, C.; Gerhauser, I. Ferrets are valuable models for SARS-CoV-2 research. *Vet Pathol.* **2022**, *59* (4), 661−672.
(39) Conforti, A.; Marra, E.; Palombo, F.; Roscilli, G.; Ravà, M.; Fumagalli, V.; Muzi, A.; Maffei, M.; Luberto, L.; Lione, L.; Salvatori, E.; Compagnone, M.; Pinto, E.; Pavoni, E.; Bucci, F.; Vitagliano, G.;

https://doi.org/10.1021/acsomega.4c03285
ACS Omega 2024, 9, 34624−34635

Stoppoloni, D.; Pacello, M. L.; Cappelletti, M.; Ferrara, F. F.; D'Acunto, E.; Chiarini, V.; Arriga, R.; Nyska, A.; Di Lucia, P.; Marotta, D.; Bono, E.; Giustini, L.; Sala, E.; Perucchini, C.; Paterson, J.; Ryan, K. A.; Challis, A. R.; Matusali, G.; Colavita, F.; Caselli, G.; Criscuolo, E.; Clementi, N.; Mancini, N.; Groß, R.; Seidel, A.; Wettstein, L.; Münch, J.; Donnici, L.; Conti, M.; De Francesco, R.; Kuka, M.; Ciliberto, G.; Castilletti, C.; Capobianchi, M. R.; Ippolito, G.; Guidotti, L. G.; Rovati, L.; Iannacone, M.; Aurisicchio, L. COVID-eVax, an electroporated DNA vaccine candidate encoding the SARS-CoV-2 RBD, elicits protective responses in animal models. *Mol. Ther.* **2022**, *30* (1), 311−326.

(40) Gupta, D.; Kumar, M.; Sharma, P.; Mohan, T.; Prakash, A.; Kumari, R.; Kaur, P. Effect of Double Mutation (L452R and E484Q) on the Binding Affinity of Monoclonal Antibodies (mAbs) against the RBD-A Target for Vaccine Development. *Vaccines (Basel).* **2023**, *11* (1), 23.

(41) Amici, A.; Pozzi, D.; Marchini, C.; Caracciolo, G. The Transformative Potential of Lipid Nanoparticle-Protein Corona for Next-Generation Vaccines and Therapeutics. *Mol. Pharmaceutics* **2023**, *20* (11), 5247−5253.

(42) Liao, H.-C.; Shen, K.-Y.; Yang, C.-H.; Chiu, F.-F.; Chiang, C.-Y.; Chai, K. M.; Huang, W.-C.; Ho, H.-M.; Chen, Y.-H.; Huang, M.-S.; Liao, C.-L.; Chen, H.-W.; Huang, M.-H.; Liu, S.-J. Lipid nanoparticle-encapsulated DNA vaccine robustly induce superior immune responses to the mRNA vaccine in Syrian hamsters. *Mol. Ther. Methods Clin. Dev.* **2024**, *32* (1), No. 101169.

(43) Quagliarini, E.; Wang, J.; Renzi, S.; Cui, L.; Digiacomo, L.; Ferri, G.; Pesce, L.; De lorenzi, V.; Matteoli, G.; Amenitsch, H.; Masuelli, L.; Bei, R.; Pozzi, D.; Amici, A.; Cardarelli, F.; Marchini, C.; Caracciolo, G. Mechanistic Insights into the Superior DNA Delivery Efficiency of Multicomponent Lipid Nanoparticles: An In Vitro and In Vivo Study. *ACS Appl. Mater. Interfaces* **2022**, *14* (51), 56666−56677.

(44) Shang, J.; Ye, G.; Shi, K.; Wan, Y.; Luo, C.; Aihara, H.; Geng, Q.; Auerbach, A.; Li, F. Structural basis of receptor recognition by SARS-CoV-2. *Nature* **2020**, *581* (7807), 221−224.

(45) Liu, H.; Naismith, J. H. An efficient one-step site-directed deletion, insertion, single and multiple-site plasmid mutagenesis protocol. *BMC Biotechnol.* **2008**, *8* (1), 91.

(46) Bartolacci, C.; Andreani, C.; Curcio, C.; Occhipinti, S.; Massaccesi, L.; Giovarelli, M.; Galeazzi, R.; Iezzi, M.; Tilio, M.; Gambini, V.; Wang, J.; Marchini, C.; Amici, A. Phage-Based Anti-HER2 Vaccination Can Circumvent Immune Tolerance against Breast Cancer. *Cancer Immunol. Res.* **2018**, *6* (12), 1486−1498.

(47) Rolla, S.; Marchini, C.; Malinarich, S.; Quaglino, E.; Lanzardo, S.; Montani, M.; Iezzi, M.; Angeletti, M.; Ramadori, G.; Forni, G.; Cavallo, F.; Augusto, A. Protective immunity against neu-positive carcinomas elicited by electroporation of plasmids encoding decreasing fragments of rat neu extracellular domain. *Hum. Gene Ther.* **2008**, *19*, 229−240.

(48) Quaglino, E.; Mastini, C.; Amici, A.; Marchini, C.; Iezzi, M.; Lanzardo, S.; De Giovanni, C.; Montani, M.; Lollini, P. L.; Masucci, G.; Forni, G.; Cavallo, F. A better immune reaction to Erbb-2 tumors is elicited in mice by DNA vaccines encoding rat/human chimeric proteins. *Cancer Res.* **2010**, *70* (7), 2604−2612.

(49) Davenport, B. J.; Morrison, T. E.; Kedl, R. M.; Klarquist, J. Conserved and Novel Mouse CD8 T Cell Epitopes within SARS-CoV-2 Spike Receptor Binding Domain Protein Identified Following Subunit Vaccination. *J. Immunol.* **2021**, *206*, 2503−2507.

(50) Malavolta, M.; Giacconi, R.; Piacenza, F.; Strizzi, S.; Cardelli, M.; Bigossi, G.; Marcozzi, S.; Tiano, L.; Marcheggiani, F.; Matacchione, G.; Giuliani, A.; Olivieri, F.; Crivellari, I.; Beltrami, A. P.; Serra, A.; Demaria, M.; Provinciali, M. Simple Detection of Unstained Live Senescent Cells with Imaging Flow Cytometry. *Cells* **2022**, *11* (16), 2506.

https://doi.org/10.1021/acsomega.4c03285
ACS Omega 2024, 9, 34624−34635